

Unifying constitutive law of vibroconvective turbulence in microgravity

Jian-Zhao Wu, Xi-Li Guo, Chao-Ben Zhao, Bo-Fu Wang,^{a)} Kai Leong Chong,^{a)} and Quan Zhou^{a)}

*Shanghai Key Laboratory of Mechanics in Energy Engineering,
Shanghai Institute of Applied Mathematics and Mechanics,
School of Mechanics and Engineering Science, Shanghai University, Shanghai,
200072, China*

The emergence of unified constitutive law is a hallmark of convective turbulence, i.e., $Nu \sim Ra^\beta$ with $\beta \approx 0.3$ in the classical and $\beta = 1/2$ in the ultimate regime, where the Nusselt number Nu measures the global heat transport and the Rayleigh number Ra quantifies the strength of thermal forcing. In recent years, vibroconvective flows have been attractive due to its ability to drive flow instability and generate “artificial gravity”, which have potential to effective heat and mass transport in microgravity. However, the existence of constitutive laws in vibroconvective turbulence remains unclear. To address this issue, we carry out direct numerical simulations in a wide range of frequencies and amplitudes, and report that the heat transport exhibits a universal scaling law $Nu \sim a^{-1} Re_{os}^\beta$ where a is the vibration amplitude, Re_{os} is the oscillational Reynolds number, and β is the universal exponent. We find that the dynamics of boundary layers plays an essential role in vibroconvective heat transport, and the Nu -scaling exponent β is determined by the competition between the thermal boundary layer (TBL) and vibration-induced oscillating boundary layer (OBL). Then a physical model is proposed to explain the change of scaling exponent from $\beta = 2$ in the OBL-dominant regime to $\beta = 4/3$ in the TBL-dominant regime. We conclude that vibroconvective turbulence in microgravity defines a distinct universality class of convective turbulence. This work elucidates the emergence of universal constitutive laws in vibroconvective turbulence, and opens up a new avenue for generating a controllable effective heat transport under microgravity or even microfluidic environment in which gravity is nearly absent.

^{a)}Authors to whom correspondence should be addressed: bofuwang@shu.edu.cn; klchong@shu.edu.cn; and qzhou@shu.edu.cn

I. INTRODUCTION

On Earth, gravity-induced turbulent convection holds a central place as its ability to vigorously transport heat in nature and industrial applications¹⁻⁴. The main challenge of convective turbulence studies is to explore the basic properties of heat transport, namely, the “constitutive law”⁴⁻⁸. The paradigmatic setup to study convective flows is the Rayleigh-Bénard (RB) convection, i.e., a fluid layer heated from below and cooled from above. The heat transport properties are then related to the scaling behavior between the dimensionless heat flux (characterized by the Nusselt number Nu) and the dimensionless temperature difference (characterized by the Rayleigh number Ra), i.e., $Nu \sim Ra^\beta$ where β is the scaling exponent. Decades of studies on RB setup show the emergence of universal scaling exponent in the constitutive law⁹⁻¹⁸. Typically, one theoretically arguments $\beta = 1/3$ from the elegant theory of marginal stability^{9,16,18}, or $\beta \approx 0.3$ from experimental observations¹³ in the classical regime, and $\beta = 1/2$ in the ultimate regime predicted by a mixing length model assuming that the heat flux is fully controlled by turbulence^{11,12}. Both heat transport scaling relations are extensively examined by various experimental and numerical investigations¹³⁻¹⁸. Grossmann and Lohse¹⁹⁻²¹ developed the unified theory, which well explains the observed heat transport scaling behaviors and successfully describes the existing experimental and numerical data.

In microgravity, as the gravity is however almost absent, gravity-induced convection becomes too feeble to transport matter and heat. Vibration, omnipresent in science and technology, has been shown to be an attractive way to operate fluids, modulate convective patterns, and control heat transport by creating an “artificial gravity”^{22,23}, e.g., vibration shapes liquid interfaces in arbitrary direction²⁴⁻²⁶, vibration levitates a fluid layer upon a gas layer²⁷, vibration selects patterns through the parametric response²⁸⁻³¹, vibration significantly enhances or suppresses heat transport depending on the mutual direction of vibration and temperature gradient³²⁻³⁵. Vibroconvection, resulting directly from a non-isothermal fluid subjected to the external vibration, is very pronounced under microgravity conditions and provides a potential mechanism of heat and mass transport in absence of gravity-induced convection³⁶⁻³⁸. Elucidating the potential constitutive law of vibroconvective turbulence and its underlying mechanism is not only of great importance in microgravity science, but also provides practical guiding significance for space missions³⁹ and microfluidic technologies^{40,41}.

In past decades, due to the difficulty of microgravity experiments, the experimental studies on vibroconvection at low gravity were limited. A known experiment was carried out with the ALICE-2 instrument onboard MIR station, which revealed the vibrational influence on the propagation of a temperature wave from a heat source in near-critical fluids^{42,43}. The other known experiment was conducted in the parabolic flights during the 46-th campaign organized by the European Space Agency, which reported the first direct experimental evidence of vibroconvection in low gravity^{37,38}. There are extensive theoretical and numerical investigations of vibroconvection under weightlessness conditions. In the limiting case of high-frequencies and small amplitudes, the averaging technique was applied to theoretically deduce the dynamical equation of the mean flows³⁶. Based on the averaged equations, the onset and bifurcation scenarios of vibroconvection were widely investigated in square, rectangular, and cubic enclosures^{44,45}. The synchronous, subharmonic and non-periodic responses to external vibration were observed in vibroconvection from a parametric study over a wide range of frequencies and amplitudes^{46,47}. The parametric and Rayleigh-vibrational instability were examined in vibroconvection in the absence of gravity^{48,49}. The heat transport enhancement near the onset of vibroconvection were also investigated^{36,38}. However, the basic properties of constitutive law in vibroconvective turbulence have been rarely addressed.

All together, one key question of whether heat transport with scaling behavior and universal exponents can exist in vibroconvective turbulence remains unclear. Here, due to the limitation of microgravity experiments, we theoretically and numerically unveil the emergence of unified constitutive law and underlying mechanism of vibroconvective turbulence. We carried out a series of direct numerical simulations on vibroconvection in a wide range of amplitudes and frequencies. We find that the thermal columns, generated by vibration-induced “artificial gravity”, are the major structures responsible to transport heat, which are different from that in gravity-induced convection, like the large-scale circulation in classical RB convection. We also find that a unified scaling law in vibroconvection indeed exists, and the scaling behavior is determined by the competition between the thermal boundary layer (TBL) and oscillating boundary layer (OBL) induced by external vibration. The heat transport scaling transits from $Nu \sim a^{-1} Re_{os}^2$ in the OBL-dominant regime to $Nu \sim a^{-1} Re_{os}^{4/3}$ in the TBL-dominant regime, where a is the vibration amplitude and Re_{os} is the oscillational Reynolds number. It is concluded that vibroconvective turbulence in microgravity defines a unified constitutive law with distinct underlying mechanism of gravity-induced convective

turbulence on Earth.

II. RESULTS

A. Flow structure

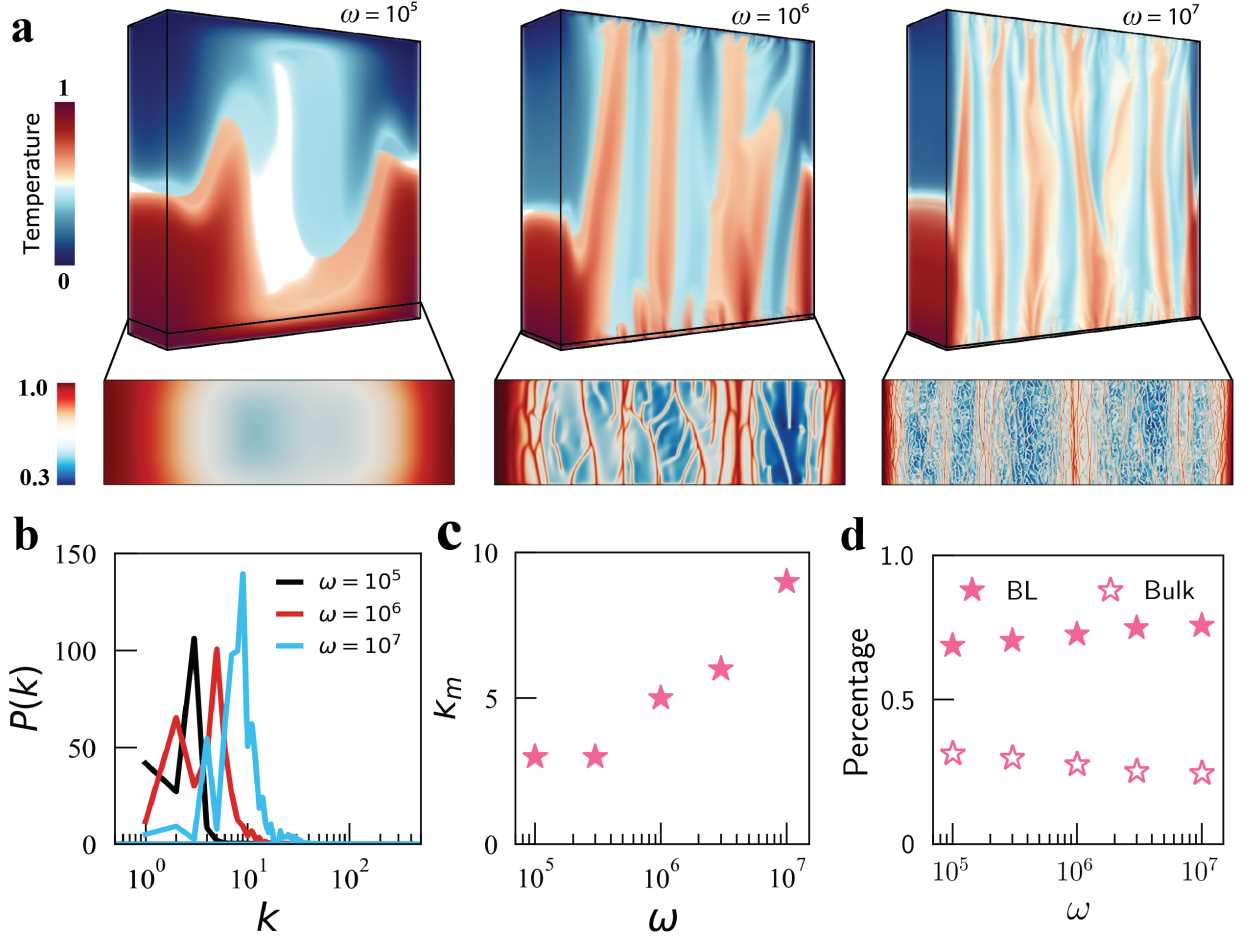


FIG. 1. **Flow structure in microgravity vibroconvection.** **a**, Instantaneous flow structure observed under different vibration frequency $\omega = 10^5$ (left), 10^6 (middle), and 10^7 (right) at fixed amplitude $a = 0.01$ and Prandtl number $Pr = 4.38$. The 3D flow structures are illustrated by the volume rendering of instantaneous temperature field (see supplementary movies). Below shows the corresponding temperature contours extracted on the horizontal slice at $z = \delta_{th}$. Here, a and ω are the dimensionless vibration amplitude and angular frequency with respect to the cell height H and the viscous diffusion time scale H^2/ν , respectively; δ_{th} denotes the thickness of thermal boundary layer. **b**, Power spectrum of fluctuating temperature in bulk zones. **c**, The variation of the characteristic wave number k_m as functions of ω . **d**, Percentage of boundary layer (BL) (solid symbols) and bulk (hollow symbols) to the global averaged thermal dissipation rate, as functions of vibration frequency ω .

The vibroconvection setup in our study is the convective flows in an enclosure heated from below by a hot wall and cooled from above by a cold wall, and subjected to the harmonic vibration in horizontal direction. All simulations reported here are of the Navier-Stokes equations of vibroconvection under Boussinesq approximation and performed in a rectangular enclosure of aspect-ratio of $W:D:H = 1:0.3:1$ in three-dimensional cases and of $W:H=1:1$ in two-dimensional cases, where W , D , H are respectively the width, depth and height of convection cell.

Figure 1a shows the typical snapshots of flow structures in vibroconvection with different dimensionless frequencies $\omega = 10^5$, 10^6 , and 10^7 at fixed dimensionless amplitude $a = 0.01$ and fixed Prandtl number $Pr = 4.38$. Here, the Prandtl number, dimensionless frequency and amplitude are defined as $Pr = \nu/\kappa$, $\omega = \Omega H^2/\nu$ and $a = \alpha \Delta A/H$, where ν , κ , α and Δ are respectively the kinematic viscosity, thermal diffusivity, thermal expansion coefficient and temperature difference between hot and cold plates; Ω and A are the angular frequency and pulsating displacement of the external vibration. It is seen that the shaking by external vibration strongly destabilizes the conductive state and generates large distortion of temperature field in bulk regions by creating an artificial gravity^{22,23}. With increasing ω , it is vibration-induced artificial gravity that becomes strong enough to destabilize thermal boundary layer and trigger abundant thermal plumes. Those plumes are transported into bulk regions and self-organized into columnar structures. This indicates that the feature of main structures responsible for heat transport in microgravity vibroconvection is different from that in the gravity-induced RB convection.

To quantitatively analyze the feature of columnar structures, we extract the instantaneous temperature field in bulk zones and calculate the power spectrum $P(k)$ of temperature fluctuations by applying the Fourier transform in the vibrational direction as shown in Fig. 1b. It is found that there exists a characteristic wave number k_m , at which the wave number distribution function $P(k)$ is maximal. Indeed, k_m characterizes the number of columnar structures in vibroconvection. We then plot the variation of k_m as functions of ω in Fig. 1c. It is shown that k_m monotonically increases with increasing ω , indicating that more columnar structures are formed under stronger vibrational driving force. This is consistent with the fact that larger heat transport enhancement occurs at larger ω . Further, to examine the role of thermal boundary layer in vibroconvective heat transport processes, we decompose the globally averaged thermal dissipation rate $\epsilon_T = \kappa |\nabla T|^2$ into their boundary

layer (BL) and bulk contributions, and then plot the variation of relative contributions as functions of ω in Fig. 1d, as suggested by the theory of Grossmann and Lohse^{19–21}. Here, T is the temperature field. It is seen in Fig. 1d that the BL contribution of ϵ_T is much larger than the bulk one, suggesting the BL-dominant thermal dissipation. This reveals that the dynamics of boundary layers plays a crucial role on the underlying mechanism of heat transport in vibroconvective turbulence.

B. Heat transport scaling

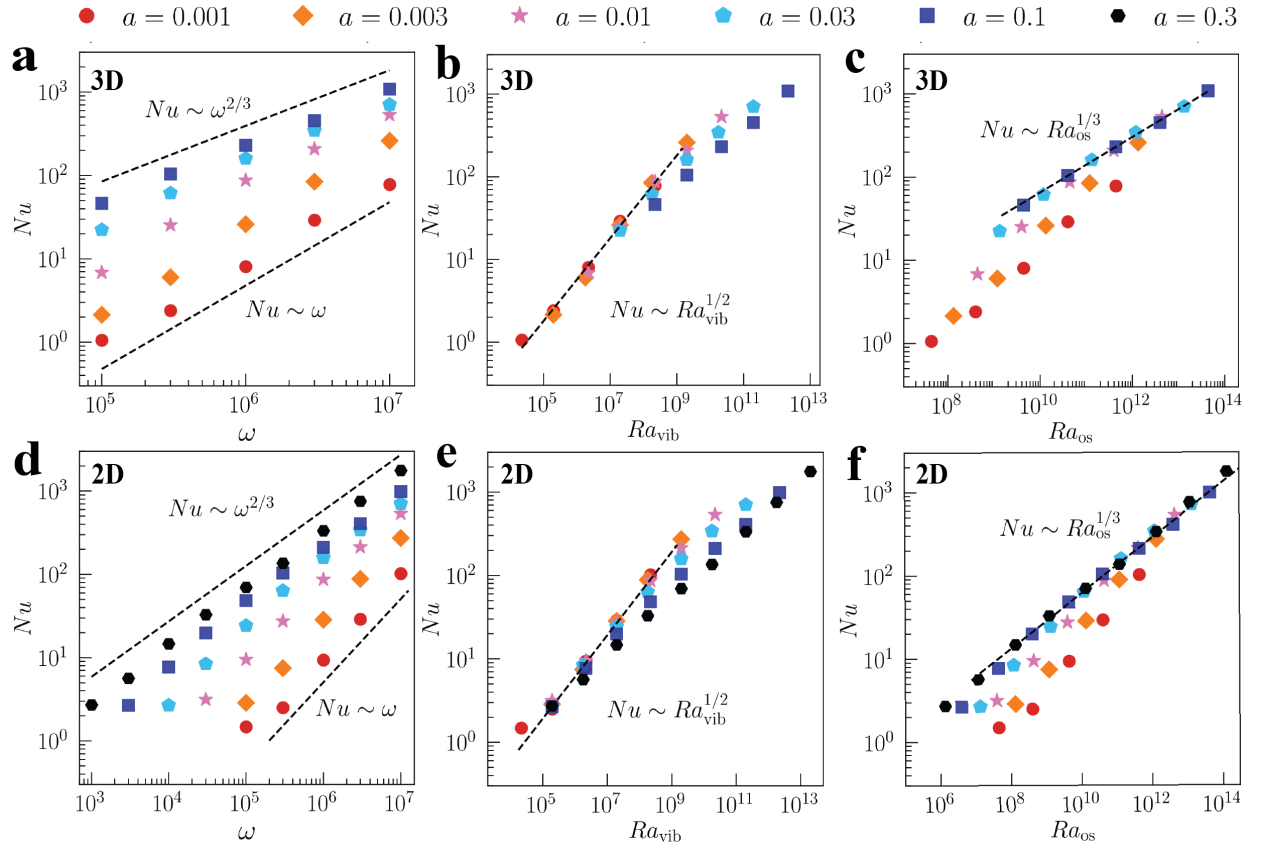


FIG. 2. Heat transport scaling in vibroconvective turbulence. **a-c**, The measured Nusselt number Nu as functions of vibration frequency ω , vibrational Rayleigh number Ra_{vib} , oscillational Rayleigh number Ra_{os} for three-dimensional (3D) cases. **d-f**, The measured Nusselt number Nu as functions of vibration frequency ω , vibrational Rayleigh number Ra_{vib} , oscillational Rayleigh number Ra_{os} for two-dimensional (2D) cases. The dashed lines in figures are $Nu \sim \omega$ (lower), $Nu \sim \omega^{2/3}$ (upper) in **a** and **d**, $Nu \sim Ra_{vib}^{1/2}$ in **b** and **e**, $Nu \sim Ra_{os}^{1/3}$ in **c** and **f**. Those precise scaling relations are theoretically deduced by a physical model proposed in subsection II C. Note that the vibration amplitude range in 3D cases is from $a = 10^{-3}$ to $a = 10^{-1}$ and in 2D cases is from $a = 10^{-3}$ to $a = 3 \times 10^{-1}$.

Given that vibroconvective flow structure is different from that in gravity-induced convection, we next address the question of how the global heat transport depends on the control parameters of vibroconvection. First, we examine the dependence of heat transport on the vibration frequency. Figures 2a,d show the measured Nu as functions of vibration frequency ω in a log-log plot for different amplitudes a in three-dimensional (3D) and two-dimensional (2D) cases. Here, the Nu number, as the nondimensional ratio of the measured heat flux to the conductive one, is calculated by $Nu = \langle wT - \kappa \partial_z T \rangle / (\kappa \Delta / H)$, where w is the vertical velocity and $\langle \cdot \rangle$ denotes the time and space averaging. It is observed that the $Nu \sim \omega^{\beta_a}$ scaling relation is not unique for different amplitudes, namely, the value of exponent β_a depends on the vibration amplitude. With increasing a , the scaling exponent decreases from $\beta_a = 1$ at $a = 10^{-3}$ to $\beta_a = 2/3$ at $a = 10^{-1}$ for 3D (at $a = 3 \times 10^{-1}$ for 2D), as shown by the dashed lines. It should be noted that the precise values of β_a are obtained from the physical model in subsection II C, not adjusted from the fitting with the numerical data.

Further, we examine the dependency of heat transport on the two important analogous Rayleigh numbers in vibroconvective turbulence, which are the vibrational Rayleigh number Ra_{vib} and oscillational Rayleigh number Ra_{os} . The first one is the vibrational Rayleigh number $Ra_{\text{vib}} = (\alpha A \Omega \Delta H)^2 / (2\nu\kappa)$, which is obtained from applying the averaged approach on vibroconvective equations in the limit of small amplitudes and high frequencies, and quantifies the intensity of the external vibrational source. Figures 2b,e depict respectively the measured Nu as functions of Ra_{vib} in a log-log plot at different amplitudes for 3D and 2D cases. We find that at small Ra_{vib} , numerical data almost collapse together on the same scaling law, i.e., $Nu \sim Ra_{\text{vib}}^{1/2}$, as shown by the dashed lines. However, at large Ra_{vib} , a significant departure from this scaling behavior is observed for large amplitudes. The other is the oscillational Rayleigh number $Ra_{\text{os}} = \alpha A \Omega^2 \Delta H^3 / (\nu\kappa)$, which is analogous to Rayleigh number in RB convection but replacing the gravitation by the vibration-induced acceleration. Figures 2c,f show the variation of Nu as functions of Ra_{os} for various amplitudes in 3D and 2D cases. We find that at large Ra_{os} , numerical data almost collapse onto the same scaling relation $Nu \sim Ra_{\text{os}}^{1/3}$ as shown by the dashed line, but at small Ra_{os} , numerical data points deviate a lot from this scaling for small amplitudes. Both $Nu \sim Ra_{\text{vib}}^{1/2}$ and $Nu \sim Ra_{\text{os}}^{1/3}$ show the independence of the cell height H , but exhibit different scaling behaviors with the intensity of vibration and the temperature difference Δ between hot and cold plates. From above, using solely the common control parameters like ω , Ra_{vib} or Ra_{os} , unifying the heat

transport scaling in vibroconvective turbulence can not be achieved.

C. Unified constitutive law

There are two important questions remaining to be answered in vibroconvective turbulence: one is why there exists two different heat transport scaling laws, i.e., $Nu \sim Ra_{\text{vib}}^{1/2}$ and $Nu \sim Ra_{\text{os}}^{1/3}$; the other is whether a unified constitutive law emerges in vibroconvective turbulence. Hereafter, we propose a physical model to address both questions and uncover underlying mechanism of heat transport.

As illustrated in subsection II A, we know that the BL-contribution to the global thermal dissipation rate is dominant, implying that the BL dynamics plays a crucial role in heat transport mechanism. In vibroconvective turbulence, there are two types of BL: the thermal boundary layer (TBL) with the thickness of δ_{th} , which is estimated by $\delta_{\text{th}} \approx H/(2Nu)$; the other is the oscillating boundary layer (OBL) induced by the external vibration. The modulation depth of OBL referring to δ_{os} is defined as the depth, at which the delaying rate of the intensity of vibration-induced shear effect equals to 99%. Considering the intensity of vibrational modulation falling off exponentially from the surface, one easily obtains $\delta_{\text{os}} = -\ln(1 - 0.99)\delta_S \approx 4.605\delta_S$ where $\delta_S = \sqrt{2\nu/\Omega}$ is the Stokes layer thickness. First, when $\delta_{\text{th}} > \delta_{\text{os}}$ as sketched in Fig. 3a above, by taking into account the balance between the convective and conductive transports within TBL, the dimensional analysis of the governing equation of temperature field gives rise to

$$w \frac{\Delta}{\delta_{\text{th}}} \sim \kappa \frac{\Delta}{\delta_{\text{th}}^2}. \quad (1)$$

And in the momentum equation, the balance between the vibration-induced buoyancy and the viscous dissipation leads to

$$\alpha A \Omega^2 \Delta \sim \nu \frac{u}{\delta_{\text{os}}^2}, \quad (2)$$

where u is the horizontal velocity. From equation (1), the thickness of TBL is found to scale as $\delta_{\text{th}} \sim \kappa w^{-1}$. From equation (2), one can obtain $u \sim \alpha A \Omega^2 \Delta \delta_{\text{os}}^2 \nu^{-1}$. Assuming that the magnitude of velocity components u and w follows a similar scaling behavior, i.e., $u \sim w$, together with $\delta_{\text{os}} \sim \sqrt{\nu/\Omega}$ and $\delta_{\text{th}} \sim H/Nu$, one obtains the scaling relation between Nu

and Ra_{vib} ,

$$Nu \sim Ra_{\text{vib}}^{1/2} Pr^{1/2}. \quad (3)$$

The scaling relation in equation (3) shows that vibroconvective heat transport is independent of viscosity ν , but depends on thermal diffusion coefficient κ . This implies that the dynamics of TBL is dominant to heat transport in cases of $\delta_{\text{th}} > \delta_{\text{os}}$.

When $\delta_{\text{th}} < \delta_{\text{os}}$ as sketched in the lower panel of Fig.3a, the balance between the vibration-induced buoyancy and the viscous dissipation within TBL allows one to rewrite the momentum equation as below using dimensional analysis

$$\alpha A \Omega^2 \Delta \sim \nu \frac{u}{\delta_{\text{th}}^2}. \quad (4)$$

Combining equations (1) and (4), together with $u \sim w$, $\delta_{\text{os}} \sim \sqrt{\nu/\Omega}$ and $\delta_{\text{th}} \sim H/Nu$, one deduces the scaling relation between Nu and Ra_{os}

$$Nu \sim Ra_{\text{os}}^{1/3}. \quad (5)$$

The heat transport scaling in equation (5) is similar to that of RB convection in the classical regime through replacing the gravitation by vibration-induced acceleration. Both heat transport scalings predicted in equations (3) and (5) agree well with numerical results shown in Fig. 2. The competition between TBL and OBL results in the two different heat transport scaling relations, namely, $Nu \sim Ra_{\text{vib}}^{1/2}$ and $Nu \sim Ra_{\text{os}}^{1/3}$.

Furthermore, we address the second question of whether the universal constitutive law of vibroconvective turbulence emerges. First, to quantify the dynamics of OBL, we define the oscillational Reynolds number $Re_{\text{os}} = \alpha \Delta A \Omega \delta_{\text{os}} / \nu$, which is related to the vibrational velocity with the Boussinesq parameter $\alpha \Delta A \Omega$ and the modulation depth δ_{os} . Second, we study the dependency of Nu on Re_{os} . It is intriguing to find that both $Nu \sim Ra_{\text{vib}}^{1/2}$ and $Nu \sim Ra_{\text{os}}^{1/3}$ scaling laws can be rewritten as $Nu \sim a^{-1} Re_{\text{os}}^\beta$ with $\beta = 2$ for the TBL-dominant heat transport regime ($\delta_{\text{th}} > \delta_{\text{os}}$), and $\beta = 4/3$ for the OBL-dominant heat transport regime ($\delta_{\text{th}} < \delta_{\text{os}}$). Therefore, we conclude that due to the competition between the dynamics TBL and OBL on heat transport, the underlying mechanism of heat transport

in vibroconvective turbulence can be categorized into two following regimes:

- (1) TBL-dominant regime ($\delta_{\text{th}} > \delta_{\text{os}}$): the OBL is submerged into TBL. Thermal plumes facilitated by vibration-induced strong shear detach from OBL and move into TBL. The plume dynamics is then mainly dominant by the molecular diffusion between OBL and TBL. Those plumes thermally diffuse and then self-organize into columnar structures in bulk zones, which transport heat from the bottom hot plate to the top cold one. The heat transport scaling exhibits the scaling $Nu \sim a^{-1} Re_{\text{os}}^2$.
- (2) OBL-dominant regime ($\delta_{\text{os}} > \delta_{\text{th}}$): the TBL is nested into OBL. The OBL dominates the dynamics of thermal plumes ejected from TBL by vibration-induced strong shear. Between OBL and TBL, the shear effect mixes those plumes and sweep away some of them^{50,51}. The remaining plumes then move into bulk zones and self-organize into columnar structures. In this regime, due to the plume-sweeping mechanism between OBL and TBL, the heat transport is depleted and obeys the scaling with a smaller scaling relation exponent $Nu \sim a^{-1} Re_{\text{os}}^{4/3}$.

Finally, we use the simulated data to confirm the theoretically deduced unified constitutive law. First, we plot in Fig. 3b,d the variation of both $a\delta_{\text{th}}$ and $a\delta_{\text{os}}$ as functions of Re_{os} . It is shown that for all fixed amplitudes, the value of both δ_{th} and δ_{os} monotonically decreases as increasing Re_{os} , and δ_{th} decreases faster than δ_{os} . The intersection point between the curves of $a\delta_{\text{th}}$ and $a\delta_{\text{os}}$ divides the the plane into two regions, which corresponds to the TBL-dominant regime in the left side ($\delta_{\text{th}} > \delta_{\text{os}}$) and OBL-dominant regime in the right side ($\delta_{\text{th}} < \delta_{\text{os}}$). As depicted in the inset of Fig. 3b,d, the dividing line between TBL-dominant and OBL-dominant regimes is nearly at the position of $\delta_{\text{os}}/\delta_{\text{th}} = 1$. This confirms that the underlying mechanism of vibroconvective heat transport is attributed to the competition between the dynamics of TBL and OBL. Second, we plot the calculated aNu as functions of Re_{os} as shown in Fig. 3c,e. It is expected that all numerical data collapse together onto the derived universal constitutive law. Evidently, the numerical data and theoretical model show an excellent agreement. This confirms the emergence of universal constitutive law of vibroconvective turbulence in microgravity.

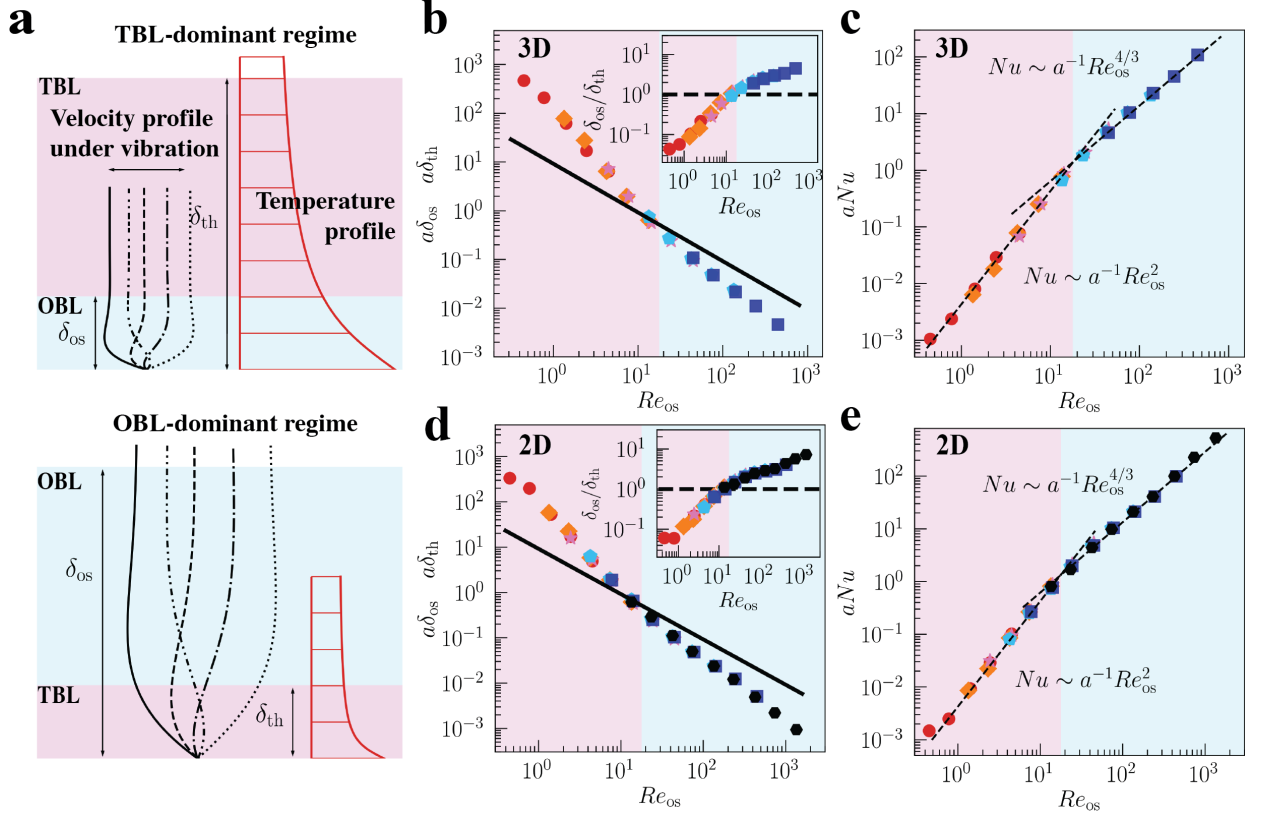


FIG. 3. **Unified constitutive law in vibroconvective turbulence.** **a**, Sketch of oscillating-boundary-layer (OBL) dominant regime and thermal-boundary-layer (TBL) dominant regime. **b,d**, The TBL thickness δ_{th} (symbols) and the critical modulation depth δ_{os} (solid line) of OBL as a function of the oscillational Reynolds number Re_{os} for 3D and 2D cases. The insets in **b** and **d** show the ratio δ_{os}/δ_{th} as a function of the oscillational Reynolds number Re_{os} . The solid dashed line indicates $\delta_{os}/\delta_{th} = 1$. **d,e**, The unified scaling law exhibited between aNu and the oscillational Reynolds number Re_{os} for 3D and 2D cases. The emergency of universal constitutive law of vibroconvective turbulence is clearly observed.

III. DISCUSSION AND CONCLUSIONS

In summary, the innovative point of our study is the reveal of the universal constitutive law in vibroconvective turbulence, which is a new class of physical mechanism to transport heat and matter in microgravity. In the absence of gravitational acceleration, vibration creates an “artificial gravity” in microgravity to destabilize thermal boundary layer (TBL) and trigger massive eruption of thermal plumes. We find that those plumes are finally self-organized into columnar structures in bulk zones to transport heat from the bottom hot plate to the top cold one. This is different from the gravity-induced convection, like Rayleigh-Bénard convection, in which large-scale circulation is formed in bulk and dominates heat

transport. By analyzing the basic properties of heat transport, we find at small vibration amplitudes, the heat transport exhibits a power-low relation with the vibrational Rayleigh number Ra_{vib} , i.e., $Nu \sim Ra_{\text{vib}}^{1/2}$; at large amplitudes, the heat transport scaling can be well described by the oscillational Rayleigh number Ra_{os} , i.e., $Nu \sim Ra_{\text{os}}^{1/3}$. Both Nu -relations shows that the global heat flux is independent of the cell height. However, vibroconvective heat transport exhibits different scaling trends with the intensity of vibration and the temperature difference between bottom and top plates, indicating that the underlying mechanism of the two Nu -relations are completely different. We also find that the BL-contribution is dominant to the global thermal dissipation rate, implying that the dynamics of boundary layer plays an essential role in vibroconvective heat transport. We then propose a physical model to theoretically deduce both Nu -scaling-relations, and explain the distinct properties of vibroconvective heat transport, based on the competition between the thermal boundary layer (TBL) and oscillating boundary layer (OBL) induced by the external vibration. To look for the universal features, we define the oscillational Reynolds number Re_{os} quantifying the dynamics of OBL, and study the dependency of heat transport on Re_{os} . Both theoretical results and numerical data shows the emergence of universal constitutive law in vibroconvective turbulence, i.e., $Nu \sim a^{-1} Re_{\text{os}}^{\beta}$, where β is the universal scaling exponent. We also find that the exponent β is determined by the relative importance between the dynamics of TBL and of OBL to heat transport, and identify $\beta = 2$ in TBL-dominant regime and $\beta = 4/3$ in OBL-dominant regime. It is concluded that the type of vibroconvective turbulence in microgravity owns a universal constitutive law with its underlying heat transport mechanism different from that in gravity-induced convective turbulence. The emergence of universal constitutive laws in vibroconvective turbulence provides a powerful basis on generating a controllable heat transport under microgravity conditions. In addition, in microfluidic environment where the effect of gravity is nearly absent, vibroconvective turbulence can provide alternative to effective heat and mass transport in a controllable manner, which surpasses the pure diffusive transport. Looking forward, we expect that our findings can be tested by experimental realizations in space station.

IV. METHODS

We consider the coupled equations of motion for the velocity field \mathbf{u} and the temperature field T in turbulent vibroconvection under the Boussinesq approximation under microgravity conditions. Horizontal harmonic vibration $A \cos(\Omega t)$ is applied on the vibroconvection system to generate heat transport. In the non-inertial frame associated to the imposed vibration, an inertial acceleration of $A\Omega^2 \cos(\Omega t)\mathbf{e}_x$ is added to the system, where \mathbf{e}_x is the unit vector in y -direction. The governing equations for vibroconvective turbulence is then can be written as

$$\nabla \cdot \mathbf{u} = 0, \quad (6)$$

$$\partial_t \mathbf{u} + (\mathbf{u} \cdot \nabla) \mathbf{u} = -\nabla p + \nu \nabla^2 \mathbf{u} - \alpha A \Omega^2 \cos(\Omega t) T \mathbf{e}_x, \quad (7)$$

$$\partial_t T + (\mathbf{u} \cdot \nabla) T = \kappa \nabla^2 T, \quad (8)$$

where p is the kinematic pressure field. All quantities studied above have been made dimensionless with respect to the cell's height H , the temperature difference across the fluid layer Δ , and the viscous diffusion velocity ν/H . Based on these choices, the relevant control parameters for the vibroconvection system are the dimensionless vibration amplitude a , the dimensionless vibration frequency ω , and the Prandtl number Pr .

The governing equations are numerically solved by a second-order finite difference code, which has been validated many times in the literature^{32,35}. At all solid boundaries, no-slip boundary conditions are applied for the velocity. At top and bottom plates, constant temperatures $\theta_{\text{top}} = 0$ and $\theta_{\text{bot}} = 1$ are given; and at all side walls, the adiabatic conditions are adopted. We performed a series of direct numerical simulations of microgravity vibroconvective turbulence over the vibration amplitude range $0.001 \leq a \leq 0.1$ and the frequency range $10^5 \leq \omega \leq 10^7$ for 3D cases, and over the vibration amplitude range $0.001 \leq a \leq 0.3$ and the frequency range $10^3 \leq \omega \leq 10^7$ for 2D cases at fixed Prandtl number $Pr = 4.38$. For all simulations, the computational mesh size is chosen to adequately resolve the dynamics both the TBL and OBL, and the time step is chosen to not only fulfil the Courant-Friedrichs-Lewy (CFL) conditions, but also resolve the time scale of one percent of the vibration period. Further details of numerical parameters are given in the Supplementary Materials.

ACKNOWLEDGMENTS

This work was supported by the Natural Science Foundation of China under Grant Nos. 11988102, 92052201, 91852202, 11825204, 12032016, 12102246, and 11972220, the Shanghai Science and Technology Program under Project No. 20ZR1419800, the Shanghai Pujiang Program under grant No. 21PJ1404400, and the China Postdoctoral Science Foundation under Grant No. 2020M681259.

AUTHOR CONTRIBUTIONS

J.-Z. Wu performed the 3D simulations and wrote the paper. X.-L. Guo performed the 2D simulations. J.-Z. Wu, C.-B. Zhao, B.-F. Wang, K. L. Chong, and Q. Zhou analyzed and interpreted the data. B.-F. Wang, K.L. Chong, and Q. Zhou supervised the project revised the paper.

COMPETING INTERESTS

The authors declare that they have no competing interests.

DATA AVAILABILITY

The data that support the findings of this study are available from the corresponding authors upon reasonable request.

REFERENCES

- ¹Niemela, J. J., Skrbek, L., Sreenivasan, K. R., Donnelly, R. J. Turbulent convection at very high Rayleigh numbers. *Nature* **404**(6780), 837–840 (2000)
- ²Sreenivasan, K.R. Turbulent mixing: A perspective. *Proceedings of the National Academy of Sciences* **116**(37), 18175–18183 (2019)
- ³Lohse, D., Xia, K.Q. Small-scale properties of turbulent Rayleigh–Bénard convection. *Annu. Rev. Fluid Mech.* **42**(1), 335–364 (2010)

- ⁴Ahlers, G., Grossmann, S., Lohse, D. Heat transfer and large scale dynamics in turbulent Rayleigh–Bénard convection. *Rev. Mod. Phys.* **81**(2), 503–537 (2009)
- ⁵Wang, Z., Mathai, V., Sun, C. Self-sustained biphasic catalytic particle turbulence. *Nat. Commun.* **10**, 3333 (2019)
- ⁶Jiang, H., Zhu, X., Wang, D., Huisman, S.G., Sun, C. Supergravitational turbulent thermal convection. *Sci. Adv.* **6**(40), 8676 (2020)
- ⁷Zhu, X., Verschoof, R.A., Bakhuis, D., Huisman, S.G., Verzicco, R., Sun, C., Lohse, D. Wall roughness induces asymptotic ultimate turbulence. *Nat. Phys.* **14**(4), 417–423 (2018)
- ⁸Lepot, S., Aumaître, S., Gallet, B. Radiative heating achieves the ultimate regime of thermal convection. *Proc. Natl. Acad. Sci. U.S.A.* **115**(36), 8937–8941 (2018)
- ⁹Malkus, W.V. The heat transport and spectrum of thermal turbulence. *Proc. R. Soc. Lond. A* **225**(1161), 196–212 (1954)
- ¹⁰Priestley, C. Convection from a large horizontal surface. *Aust. J. Phys.* **7**(1), 176–201 (1954)
- ¹¹Kraichnan, R.H. Turbulent thermal convection at arbitrary Prandtl number. *Phys. Fluids* **5**(11), 1374–1389 (1962)
- ¹²Spiegel, E.A. A generalization of the mixing-length theory of turbulent convection. *Astrophys. J.* **138**, 216 (1963)
- ¹³Castaing, B., Gunaratne, G., Heslot, F., Kadanoff, L., Libchaber, A., Thomae, S., Wu, X.-Z., Zaleski, S., Zanetti, G. Scaling of hard thermal turbulence in Rayleigh–Bénard convection. *J. Fluid Mech.* **204**, 1–30 (1989)
- ¹⁴He, X., Funfschilling, D., Nobach, H., Bodenschatz, E., Ahlers, G. Transition to the ultimate state of turbulent Rayleigh–Bénard convection. *Phys. Rev. Lett.* **108**(2), 024502 (2012)
- ¹⁵Toppaladoddi, S., Succi, S., Wettlaufer, J.S. Roughness as a route to the ultimate regime of thermal convection. *Phys. Rev. Lett.* **118**(7), 074503 (2017)
- ¹⁶Plumley, M., Julien, K. Scaling laws in Rayleigh–Bénard convection. *Earth Space Sci.* **6**(9), 1580–1592 (2019)
- ¹⁷Iyer, K.P., Scheel, J.D., Schumacher, J., Sreenivasan, K.R. Classical 1/3 scaling of convection holds up to $Ra = 10^{15}$. *Proc. Natl. Acad. Sci. U.S.A.* **117**(14), 7594–7598 (2020)
- ¹⁸Ahlers, G., Bodenschatz, E., Hartmann, R., He, X., Lohse, D., Reiter, P., Stevens, R.J., Verzicco, R., Wedi, M., Weiss, S., *et al.* Aspect ratio dependence of heat transfer in a

- cylindrical Rayleigh-Bénard cell. *Phys. Rev. Lett.* **128**(8), 084501 (2022)
- ¹⁹Grossmann, S., Lohse, D. Scaling in thermal convection: A unifying theory. *J. Fluid Mech.* **407**, 27–56 (2000)
- ²⁰Grossmann, S., Lohse, D. Thermal convection for large Prandtl numbers. *Phys. Rev. Lett.* **86**(15), 3316 (2001)
- ²¹Stevens, R.J., van der Poel, E.P., Grossmann, S., Lohse, D. The unifying theory of scaling in thermal convection: the updated prefactors. *J. Fluid Mech.* **730**, 295–308 (2013)
- ²²Beysens, D. Vibrations in space as an artificial gravity? *Europhys. news* **37**(3), 22–25 (2006)
- ²³Beysens, D., Chatain, D., Evesque, P., Garrabos, Y. High-frequency driven capillary flows speed up the gas-liquid phase transition in zero-gravity conditions. *Phys. Rev. Lett.* **95**(3), 034502 (2005)
- ²⁴Sánchez, P.S., Gaponenko, Y., Yasnou, V., Mialdun, A., Porter, J., Shevtsova, V. Effect of initial interface orientation on patterns produced by vibrational forcing in microgravity. *J. Fluid Mech.* **884** (2020)
- ²⁵Sánchez, P.S., Yasnou, V., Gaponenko, Y., Mialdun, A., Porter, J., Shevtsova, V. Interfacial phenomena in immiscible liquids subjected to vibrations in microgravity. *J. Fluid Mech.* **865**, 850–883 (2019)
- ²⁶Apffel, B., Hidalgo-Caballero, S., Eddi, A., Fort, E. Liquid walls and interfaces in arbitrary directions stabilized by vibrations. *Proc. Natl. Acad. Sci. U.S.A.* **118**(48) (2021)
- ²⁷Apffel, B., Novkoski, F., Eddi, A., Fort, E. Floating under a levitating liquid. *Nature* **585**(7823), 48–52 (2020)
- ²⁸Rogers, J.L., Schatz, M.F., Bougie, J.L., Swift, J.B. Rayleigh-Bénard convection in a vertically oscillated fluid layer. *Phys. Rev. Lett.* **84**(1), 87 (2000)
- ²⁹Rogers, J.L., Schatz, M.F., Brausch, O., Pesch, W. Superlattice patterns in vertically oscillated Rayleigh-Bénard convection. *Phys. Rev. Lett.* **85**(20), 4281 (2000)
- ³⁰Pesch, W., Palaniappan, D., Tao, J., Busse, F.H. Convection in heated fluid layers subjected to time-periodic horizontal accelerations. *J. Fluid Mech.* **596**, 313–332 (2008)
- ³¹Salgado Sánchez, P., Gaponenko, Y.A., Porter, J., Shevtsova, V. Finite-size effects on pattern selection in immiscible fluids subjected to horizontal vibrations in weightlessness. *Phys. Rev. E* **99**, 042803 (2019).
- ³²Wang, B.-F., Zhou, Q., Sun, C. Vibration-induced boundary-layer destabilization achieves

- massive heat-transport enhancement. *Sci. Adv.* **6**(21), 8239 (2020)
- ³³Swaminathan, A., Garrett, S.L., Poese, M.E., Smith, R.W. Dynamic stabilization of the Rayleigh-Bénard instability by acceleration modulation. *J. Acoust. Soc. Am.* **144**(4), 2334–2343 (2018)
- ³⁴Wu, J.-Z., Dong, Y.-H., Wang, B.-F., Zhou, Q. Phase decomposition analysis on oscillatory Rayleigh-Bénard turbulence. *Phys. Fluids* **33**(4), 045108 (2021)
- ³⁵Wu, J.-Z., Wang, B.-F., Chong, K.L., Dong, Y.-H., Sun, C., Zhou, Q. Vibration-induced ‘anti-gravity’ tames thermal turbulence at high Rayleigh numbers. *J. Fluid Mech.* **951**, 13 (2022)
- ³⁶Gershuni, G.Z., Lyubimov, D.V. *Thermal Vibrational Convection*. Wiley & Sons, New York (1998)
- ³⁷Mialdun, A., Ryzhkov, I., Melnikov, D., Shevtsova, V. Experimental evidence of thermal vibrational convection in a nonuniformly heated fluid in a reduced gravity environment. *Phys. Rev. Lett.* **101**(8), 084501 (2008)
- ³⁸Shevtsova, V., Ryzhkov, I.I., Melnikov, D.E., Gaponenko, Y.A., Mialdun, A. Experimental and theoretical study of vibration-induced thermal convection in low gravity. *J. Fluid Mech.* **648**, 53–82 (2010)
- ³⁹Monti, R., Savino, R., Lappa, M. On the convective disturbances induced by g-jitter on the space station. *Acta Astronaut.* **48**(5-12), 603–615 (2001)
- ⁴⁰Daniel, S., Chaudhury, M.K., De Gennes, P.-G. Vibration-actuated drop motion on surfaces for batch microfluidic processes. *Langmuir* **21**(9), 4240–4248 (2005)
- ⁴¹Brunet, P., Eggers, J., Deegan, R.D. Vibration-induced climbing of drops. *Phys. Rev. Lett.* **99**, 144501 (2007).
- ⁴²Zyuzgin, A., Ivanov, A., Polezhaev, V., Putin, G., Soboleva, E. Convective motions in near-critical fluids under real zero-gravity conditions. *Cosmic Res.* **39**(2), 175–186 (2001)
- ⁴³Garrabos, Y., Beysens, D., Lecoutre, C., Dejoan, A., Polezhaev, V., Emelianov, V. Thermoconvective phenomena induced by vibrations in supercritical SF₆ under weightlessness. *Phys. Rev. E* **75**(5), 056317 (2007)
- ⁴⁴Savino, R., Monti, R., Piccirillo, M. Thermovibrational convection in a fluid cell. *Comput. Fluids* **27**(8), 923–939 (1998)
- ⁴⁵Cissé, I., Bardan, G., Mojtabi, A. Rayleigh-Bénard convective instability of a fluid under high-frequency vibration. *Int. J. Heat Mass Tran.* **47**(19-20), 4101–4112 (2004)

- ⁴⁶Hirata, K., Sasaki, T., Tanigawa, H. Vibrational effects on convection in a square cavity at zero gravity. *J. Fluid Mech.* **445**, 327–344 (2001)
- ⁴⁷Crewdson, G., Lappa, M. Thermally-driven flows and turbulence in vibrated liquids. *Int. J. Thermofluids* **11**, 100102 (2021)
- ⁴⁸Amiroudine, S., Beysens, D. Thermovibrational instability in supercritical fluids under weightlessness. *Phys. Rev. E* **78**(3), 036325 (2008)
- ⁴⁹Sharma, D., Erriguible, A., Gandikota, G., Beysens, D., Amiroudine, S. Vibration-induced thermal instabilities in supercritical fluids in the absence of gravity. *Phys. Rev. Fluids* **4**(3), 033401 (2019)
- ⁵⁰Scagliarini, A., Gylfason, Á., Toschi, F. Heat-flux scaling in turbulent Rayleigh-Bénard convection with an imposed longitudinal wind. *Phys. Rev. E* **89**(4), 043012 (2014)
- ⁵¹Blass, A., Zhu, X., Verzicco, R., Lohse, D., Stevens, R.J. Flow organization and heat transfer in turbulent wall sheared thermal convection. *J. Fluid Mech.* **897**, 22 (2020)